

# INFLUENCE OF RANDOM FLUCTUATIONS IN THE $\Lambda$ -EFFECT ON MERIDIONAL FLOW AND DIFFERENTIAL ROTATION

MATTHIAS REMPEL

High Altitude Observatory, National Center for Atmospheric Research\* , P.O. Box 3000, Boulder, Colorado 80307, USA  
*Draft version September 23, 2021*

## ABSTRACT

We present a mean field model based on the approach taken by Rempel (2005) in order to investigate the influence of stochastic fluctuations in the Reynolds stresses on meridional flow and differential rotation. The stochastic fluctuations found in the meridional flow pattern directly resemble the stochastic fluctuations of the Reynolds stresses, while the stochastic fluctuations in the differential rotation are smaller by almost two orders of magnitude. It is further found that the correlation length and time scale of the stochastic fluctuations have only a weak influence on meridional flow, but a significant influence on the magnitude of variations in the differential rotation. We analyze the energy fluxes within the model to estimate time scales for the replenishment of differential rotation and meridional flow. We find that the time scale for the replenishment of differential rotation ( $\sim 10$  years) is nearly four orders of magnitude longer than the time scale for the replenishment of meridional flow, which explains the differences in the response to stochastic fluctuations of the Reynolds stress found for both flow fields.

*Subject headings:* Sun: interior — rotation

## 1. INTRODUCTION

Recently Rempel (2005) presented a mean field model for solar differential rotation and meridional flow, assuming a parameterization of all convective scale processes, most importantly the turbulent angular momentum transport ( $\Lambda$ -effect) introduced by Kitchatinov & Rüdiger (1993). The model presented by Rempel (2005) and also other mean field models for differential rotation (see e.g. Kitchatinov & Rüdiger 1995; Rüdiger et al. 1998; Küker & Stix 2001) use a time independent parameterization of the turbulent angular momentum transport leading to stationary solutions describing the mean flows. On the other hand, 3D numerical simulations show a significant temporal variation of meridional flow and differential rotation due to the fluctuations in the convective motions leading to the Reynolds stresses (Miesch et al. 2000; Brun & Toomre 2002).

Observations of differential rotation are usually based on 3 to 4 month sets of data and therefore can only tell us something about variations on time scales longer than this period (Schou et al. 2002). The  $1\sigma$  error-intervals of inversions within the convection zone are typically around a few nHz or less than 1% of the rotation rate. The differential rotation also shows a systematic cycle variation, the torsional oscillations, which have an amplitude of around 1% of the rotation rate. By contrast the variability found in observations of the meridional surface flows is much larger compared to the average amplitude. Over time scales of years Zhao & Kosovichev (2004) found variations of the meridional surface flow of the order of  $10\text{ms}^{-1}$  compared to a mean flow amplitude of  $20\text{ms}^{-1}$ . While these variations are most probably also related to the solar cycle, much less is known about short term variations, which could be related to the turbulent

origin of the flow itself. Comparison of the long term variations found in differential rotation and meridional flow indicates that the relative amplitude of the meridional flow variability is almost a factor of 100 larger than the variability of the differential rotation.

In this paper we present a mean field model for differential rotation and meridional flow following the approach described in Rempel (2005) to investigate the influence of stochastic fluctuations in the Reynolds stresses on meridional flow and differential rotation. The main intention of this paper is to investigate how much variability can be expected in the meridional flow pattern, given the strong constraints set by helioseismology on the variability of the 3 to 4 month mean of the differential rotation. The possible influence of the solar cycle on both flow patterns will be addressed later in a separate paper.

## 2. MODEL

For this investigation we use the model described in detail in Rempel (2005). We add random noise with defined correlation length and time scales to the parameterization of the turbulent Reynolds stress responsible for driving the differential rotation and meridional flow [see Rempel (2005), equations (31) and (32)]:

$$\Lambda_{r\phi} = \Lambda_{\phi r} = +L(r, \theta) \cos(\theta + \lambda(r, \theta)) (1 + c \zeta_r(r, \theta)/\sigma_r) \quad (1)$$

$$\Lambda_{\theta\phi} = \Lambda_{\phi\theta} = -L(r, \theta) \sin(\theta + \lambda(r, \theta)) (1 + c \zeta_\theta(r, \theta)/\sigma_\theta) \quad (2)$$

$L(r, \theta)$  denotes the mean amplitude of the turbulent angular momentum flux, whereas  $\lambda(r, \theta)$  describes the mean inclination of the flux vector with respect to the axis of rotation.  $L(r, \theta)$  and  $\lambda(r, \theta)$  need to be antisymmetric across the equator to fulfill the symmetry constraints of the  $\Lambda$ -effect. For further details, see Rempel (2005).

$\zeta_r$  and  $\zeta_\theta$  denote random functions, which will be described below in more detail. The parameter  $c$  determines the amplitude of the random noise in units of the

\*The National Center for Atmospheric Research is sponsored by the National Science Foundation  
 Electronic address: rempel@hao.ucar.edu

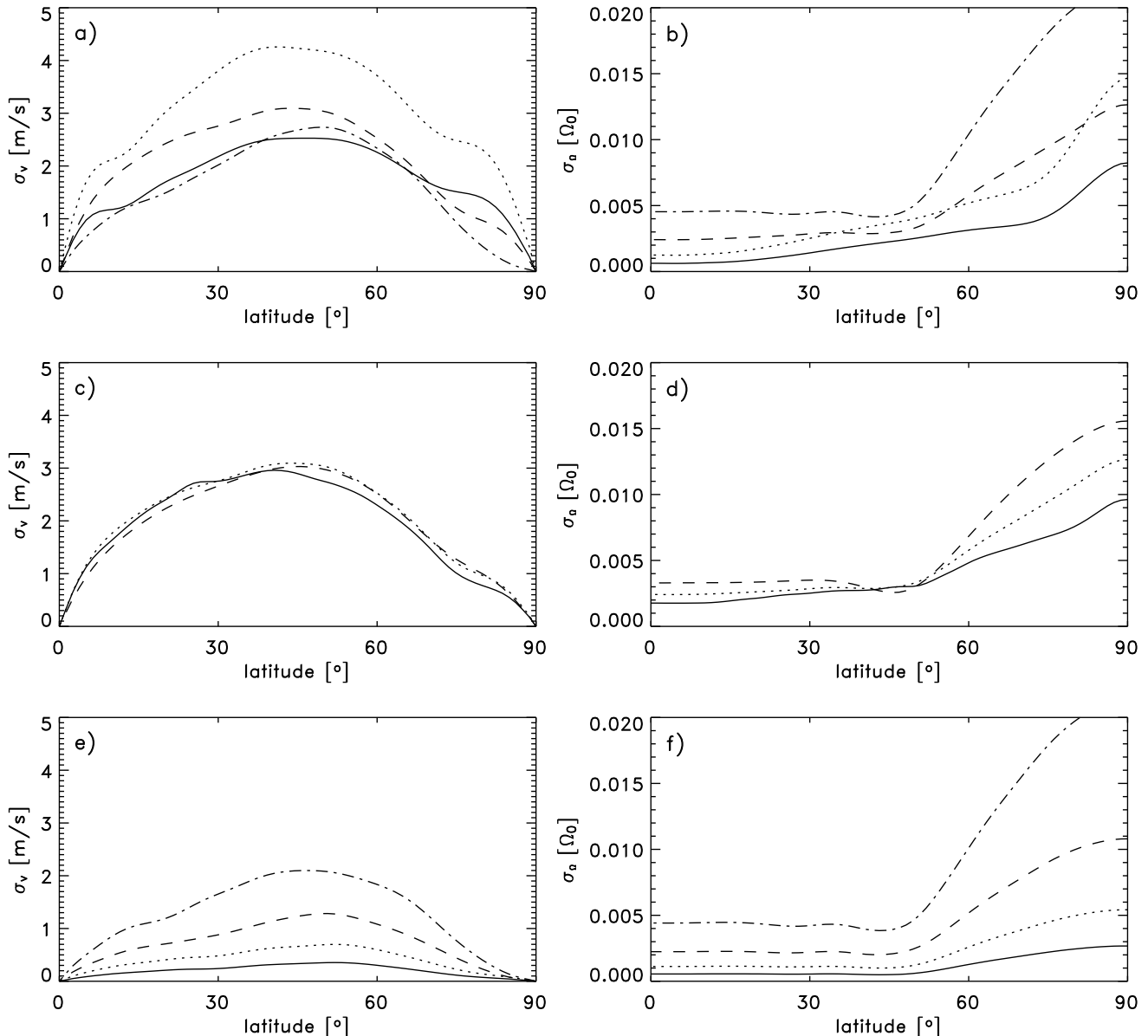


FIG. 1.— Variance of meridional flow (left panels) and differential rotation (right panels) at the top of the domain  $r = 0.985R_{\odot}$ . The top panels a) and b) show the total variance of the time series for the cases 1 to 4 (variation of correlation time scale). The solid line indicates case 1 ( $\tau = 0.25\Omega_0^{-1}$ ), the dotted line case 2 ( $\tau = 1\Omega_0^{-1}$ ), the dashed line case 3 ( $\tau = 4\Omega_0^{-1}$ ), and dashed-dotted line 4 ( $\tau = 16\Omega_0^{-1}$ ). The middle panels c) and d) show cases 5, 3, and 6 (variation of correlation length scale). The solid line indicates case 5 ( $\Delta = 0.05$ ), the dotted line case 3 ( $\Delta = 0.1$ ), and the dashed line case 6 ( $\Delta = 0.2$ ). The bottom panels e) and f) are similar to the top panels, however the variances are computed from a four month mean.

standard deviations  $\sigma_r$  and  $\sigma_{\theta}$ . By perturbing both components of the turbulent angular momentum flux with uncorrelated random functions we allow for a change of amplitude and direction of the angular momentum flux.

In order to generate a random function with a defined correlation length scale, we construct a 2D random field in the  $r$ - $\theta$ -plane by superposing Gaussian functions with a fixed width that determines the length scale. The position in the  $r$ - $\theta$ -plane of individual Gaussian as well as the amplitudes are random. We introduce a correlation time scale into the problem by performing a temporal average over the 2D random fields. In principle this averaging could be done by creating a long time series of a

2D random field and using then a running mean. However, this approach would require a fairly large amount of memory. Instead we produce a 2D random field  $g$  each time step and solve the following equation to introduce a correlations time scale:

$$\frac{\partial \zeta}{\partial t} = -\frac{\zeta}{\tau_c} + \frac{g}{\tau_c}, \quad (3)$$

where  $\zeta$  denotes the random field with a correlation time scale  $\tau_c$ . The main disadvantage of this approach is that the temporal average is always dominated by the most recent realizations of  $g$ . This effect can be reduced by

TABLE 1  
PARAMETERS FOR THE  
STOCHASTIC  
PERTURBATIONS

case	$\tau_c [\Omega_0^{-1}]$	$\Delta$
1	0.25	0.1
2	1.0	0.1
3	4.0	0.1
4	16.0	0.1
5	4.0	0.05
6	4.0	0.2

NOTE. — Models 1 to 4 cover a range in the correlation time scale by a factor of 64, whereas models 5, 3, and 6 cover correlation lengths scales varying by a factor of 4.  $\Omega_0$  denotes the rotation rate of the solar interior.

applying this method recursively as follows:

$$\begin{aligned}
 \frac{\partial \zeta_1}{\partial t} &= -\frac{\zeta_1}{\tau_c/n} + \frac{\zeta_2}{\tau_c/n} \\
 \frac{\partial \zeta_2}{\partial t} &= -\frac{\zeta_2}{\tau_c/n} + \frac{\zeta_3}{\tau_c/n} \\
 &\dots \\
 &\dots \\
 \frac{\partial \zeta_n}{\partial t} &= -\frac{\zeta_n}{\tau_c/n} + \frac{g}{\tau_c/n}, \quad (4)
 \end{aligned}$$

where  $\zeta_1$  is the random field used for the simulation. The functions  $\zeta_2$  to  $\zeta_n$  are auxiliary functions required for the averaging process. The results presented in this paper are obtained using a value of  $n = 5$  for the temporal averaging. The free parameters in this approach for generating a 2D random field are the correlation length scale  $\Delta$  and the correlation time scale  $\tau_c$ .  $\Delta$  measures the half width of the Gaussians at half maximum in units of the domain size in the radial and latitudinal direction (therefore radial and latitudinal width are not the same). For the results presented here we use an amplitude [defined by the parameter  $c$  in equations (1) and (2)] of 0.33, meaning the stochastic fluctuation imposed on the Reynolds stress has a  $1\sigma$  fluctuation corresponding to 33% of the mean.

In order to allow for a detailed statistical analysis of meridional flow and differential rotation, we compute during the simulation averages of all variables and the square of all variables over the output sampling period, which allows computing the mean flows and the standard deviations including all simulation time steps and therefore avoiding the influence of the output sampling.

### 3. RESULTS

For evaluating the effect of random noise in the turbulent angular momentum transport we use the model described in the case 1 of Rempel (2005) as reference. Table 1 summarizes the parameters we use for the generation of the random noise fields used to randomize the Reynolds stress according to equations (1) and (2). All other model parameters are given in Rempel (2005). The

cases 1 to 4 cover a range in the correlation time scale by a factor of 64 (from roughly one day to two months), while the series of cases 5, 3, and 6 encompasses a variation in the correlation length scale of a factor of 4 (from a radial half width of about 10 Mm to 40 Mm).

In the following discussion we will focus on the variance of the meridional flow  $\sigma_v$  and the variance of the differential rotation  $\sigma_\Omega$ . Since helioseismic measurements of differential rotation typically involve 4 month averages, we also compute the variance of 4 month averages of our model output.

Figure 1 shows  $\sigma_v$  (left column) and  $\sigma_\Omega$  (right column) computed at the top of the domain ( $r = 0.985R_\odot$ ) for the models 1 to 6 listed in Table 1. The top panels show the total variability for the cases 1 to 4 (change of correlation time scale), while the middle panels show the cases 5, 3, and 6 (variation of correlation length scale). The bottom panels show the same properties as the top panels, but computed from a four month mean.

The most striking feature visible in panels a) to d) is that while the fluctuations of the meridional flow show no systematic variation with correlation time and length, the fluctuations of differential rotation show a systematic increase with both. An exception is case 2 in panel a) and b), since  $\tau_c = \Omega_0^{-1}$  is very close to the time scale of inertial oscillations and therefore  $\sigma_v$  is enhanced because of a resonance. The amplitude of  $\sigma_v$  is about 20% to 25% of the mean meridional flow (in our model the meridional flow reaches a peak value of around  $13.5 \text{ ms}^{-1}$  at  $45^\circ$  latitude), which is close to the noise level added to the Reynolds stress (33%). On the other hand, except for high latitudes the value of  $\sigma_\Omega$  is less than 1% of the reference rotation rate in all cases.

Panels e) and f) show the similar quantities as panels a) and b), however computed from a four month mean of the time series, similar to the averaging interval typically used in GONG/MDI inversions of differential rotation profiles. It is not surprising that the amplitude of the fluctuations decreases, however the effect is stronger in case of the meridional flow, e.g. the averaging decreases  $\sigma_v$  for case 3 (dashed line) by a factor of 2, while  $\sigma_\Omega$  is nearly unaffected.

So far we focused on the variability of meridional flow and differential rotation at the top of the domain. Figure 2 shows the depth dependence for the meridional flow at  $45^\circ$  and the for differential rotation at the selected latitudes  $0^\circ$ ,  $15^\circ$ ,  $30^\circ$ ,  $45^\circ$ ,  $60^\circ$ , and  $90^\circ$ . In both cases solid lines indicate the mean and the grey shade the  $1\sigma$  interval. Shown is case 3 with a correlation time scale of  $4\Omega_0^{-1}$ . Both  $\sigma_v$  and  $\sigma_\Omega$  show a maximum at the top of the domain and a nearly monotonic decrease towards the base of the convection zone. We emphasize that this result was obtained by using a constant correlation time and length scale throughout the convection zone. In a more realistic description it can be expected that both correlation time and length scale decrease towards the solar surface, which according to the trends found in Figure 1 would lead to a decrease of  $\sigma_\Omega$  close to the surface, while  $\sigma_v$  remains more or less unchanged (except for the enhancement of the signal close to the resonance). In our investigation we also use a constant amplitude of the stochastic fluctuations of the Reynolds stress throughout the convection zone. A depth depen-

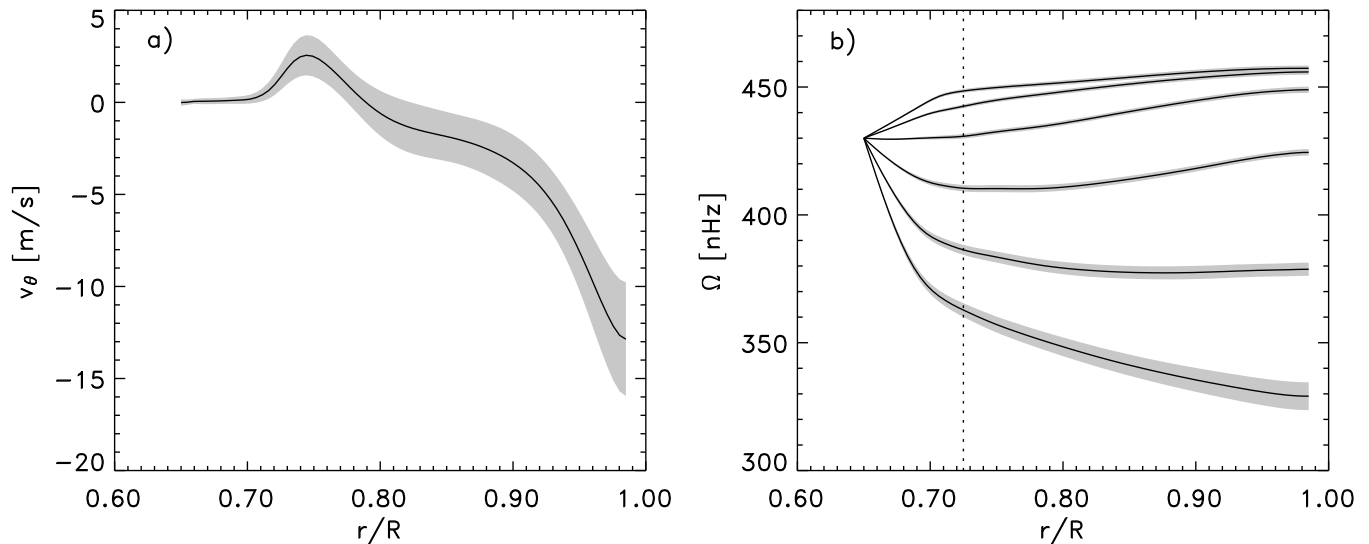


FIG. 2.— Depth variation of the standard variations of meridional flow and differential rotation for case 3. Panel a) shows the meridional flow profile at 45° latitude and the 1 $\sigma$  intervals as grey shade. Panel b) shows the differential rotation at 0°, 15°, 30°, 45°, 60°, and 90° latitude with 1 $\sigma$  intervals as grey shade.

dence of this amplitude would influence both,  $\sigma_v$  and  $\sigma_\Omega$  in a similar way.

We computed all models shown in this paper with an amplitude of  $c = 0.33$  for the random noise in the  $\Lambda$ -effect. Note that  $\sigma_v$  and  $\sigma_\Omega$  scale linearly with  $c$ , meaning that the results given here can be rescaled to apply to a different amplitude of the random noise.

We indicated already above that the variance of the meridional flow and differential rotation is enhanced around  $\tau_c \sim \Omega_0^{-1}$  because of the excitation of inertia oscillations. Figure 3 shows the variances of meridional flow and differential rotation at the top of the domain ( $r = 0.985 R_\odot$ ) for the latitudes 22.5° (solid), 45° (dotted), and 67.5° (dashed) as function of  $\tau_c$ . Panel a) shows the total variance of the meridional flow, clearly indicating a resonance around  $\tau_c \sim 1 - 2\Omega_0^{-1}$ . Since our time scale  $\tau_c$  is defined as an e-folding time scale for the random perturbations, we expect this resonance around  $\tau_c \approx \tau_i/2 = \pi/\omega_i$ , with the frequency of inertia oscillations given by  $\omega_i = 2\Omega_0$ . This leads to a locations of the resonance around

$$\tau_r \approx \frac{\pi}{2\Omega_0}. \quad (5)$$

Figure 3a shows a weak tendency of increasing  $\tau_r$  with decreasing latitude, which indicates that the geometry of the problem and the stratification leads to some confinement of motions in latitude (for motions in latitude only we would have  $\omega_i = 2\Omega_0 \cos \theta$ ).

The resonance also affects the variance of the differential rotation; however, this influence is much weaker and disappears at low latitudes (variations in the meridional flow have less influence on  $\Omega$  close to the equator). The resonance is not visible in the variance of the four month mean flows (panels c, d), which shows the monotonic increase of the  $\sigma_v$  and  $\sigma_\Omega$  with  $\tau_c$  at all latitudes as already indicated in Figure 1.

#### 4. INTERPRETATION

Our main results presented can be understood in terms of different response time scales of meridional flow and differential rotation with respect to changes in the Reynolds stress. The difference in the response time scale follows from the different size of the kinetic energy reservoirs associated with meridional flow and differential rotation. Here we make a detailed analysis of the energy fluxes within the differential rotation model in order to estimate typical time scales related to the meridional flow and differential rotation. In the following derivation we use the assumptions  $\varrho_1 \ll \varrho_0$ ,  $p_1 \ll p_0$ , and  $|\delta| = |\nabla - \nabla_{\text{ad}}| \ll 1$ . We also omit terms proportional to  $\text{div}(\varrho_0 \mathbf{v}_m)$ , which are very small for the low Mach number meridional flow and vanish for the stationary solution finally considered. We start from equations (2) to (4) of Rempel (2005) to derive two separate energy equations for the meridional flow and differential rotation. To this end we multiply equation (2) by  $\varrho_0 v_r$  and equation (3) by  $\varrho_0 v_\theta$  and add both equations. Rearrangement of the different terms leads to:

$$\begin{aligned} \frac{\partial}{\partial t} \left( \varrho_0 \frac{v_m^2}{2} \right) + \text{div} \mathbf{F}_m = & -(r \sin \theta)^2 \varrho_0 \mathbf{v}_m \cdot \text{grad} \frac{\Omega^2}{2} \\ & - \frac{1}{2} [R_{rr} E_{rr} + 2R_{r\theta} E_{r\theta} + R_{\theta\theta} E_{\theta\theta} + R_{\phi\phi} E_{\phi\phi}] \\ & + v_r \varrho_0 g \frac{s_1}{\gamma} \end{aligned} \quad (6)$$

with the energy flux:

$$\begin{aligned} \mathbf{F}_m = & \varrho_0 \mathbf{v}_m \left( \frac{v_m^2}{2} + \frac{p_1}{\varrho_0} \right) - \varrho_0 \mathbf{v}_m (r \sin \theta)^2 \frac{\Omega^2 - \Omega_0^2}{2} \\ & + \mathbf{R} \cdot \mathbf{v}_m. \end{aligned} \quad (7)$$

Here  $\mathbf{R}$  denotes the Reynolds stress tensor,  $\mathbf{E}$  the deformations tensor. For the definition we refer to Rempel (2005). Multiplying equation (4) of Rempel (2005) by  $\varrho_0 (r \sin \theta)^2 \Omega$  leads to:

$$\frac{\partial}{\partial t} \left( \varrho_0 \frac{(\Omega r \sin \theta)^2}{2} \right) + \text{div} \mathbf{F}_\Omega =$$

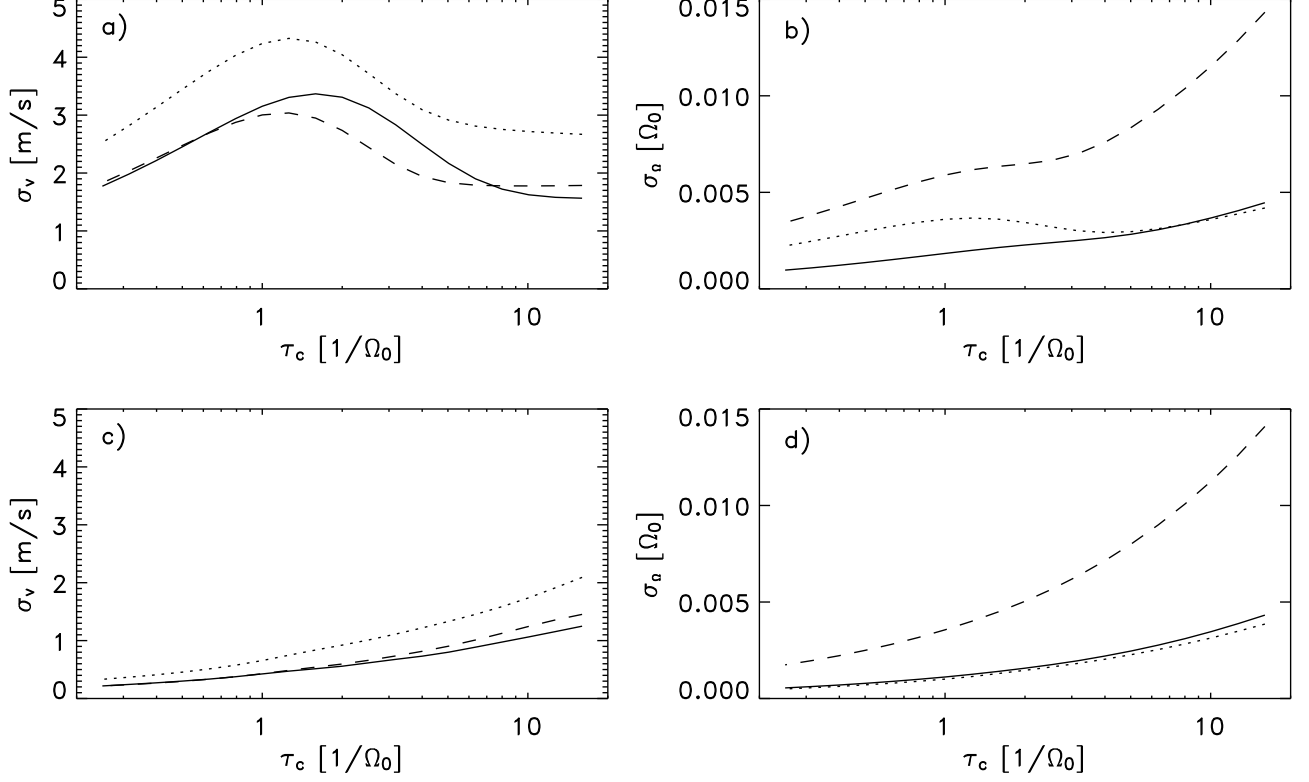


FIG. 3.— Variation of the standard variations of meridional flow and differential rotation with correlation time scale  $\tau_c$  of the random forcing. Panels (a - b) show the total variance of the time series as function of  $\tau_c$  at the top of the domain for the latitudes  $22.5^\circ$  (solid),  $45^\circ$  (dotted), and  $67.5^\circ$  (dashed). Panels (c - d) show the variance of the 4 month mean for the same variables. The enhancement of the variance caused by inertia oscillations is clearly visible in panels (a, b), but not in the four month mean shown in panels (c, d).

$$\begin{aligned}
 & -\nu_t \varrho_0 (r \sin \theta)^2 \left[ \left( \frac{\partial \Omega}{\partial r} \right)^2 + \left( \frac{1}{r} \frac{\partial \Omega}{\partial \theta} \right)^2 \right] \\
 & -\nu_t \varrho_0 r \sin \theta \left( \frac{\partial \Omega}{\partial r} \Lambda_{r\phi} + \frac{1}{r} \frac{\partial \Omega}{\partial \theta} \Lambda_{\theta\phi} \right) \\
 & + (r \sin \theta)^2 \varrho_0 \mathbf{v}_m \cdot \text{grad} \frac{\Omega^2}{2}
 \end{aligned} \quad (8)$$

with the energy flux:

$$\mathbf{F}_\Omega = \varrho_0 \mathbf{v}_m (\Omega r \sin \theta)^2 - r \sin \theta \Omega \mathbf{R}_\phi. \quad (9)$$

Here  $\mathbf{R}_\phi$  denotes a vector with components  $R_{r\phi}$  and  $R_{\theta\phi}$ . Since for the boundary conditions we use, the energy fluxes [equations (7) and (9)] vanish at the boundaries, the divergence terms in equations (6) and (8) do not contribute after integration over the entire domain, leading to the energy balances:

$$\frac{\partial E_m}{\partial t} = Q_C + Q_{visc}^m + Q_B^m, \quad (10)$$

$$\frac{\partial E_\Omega}{\partial t} = -Q_C + Q_{visc}^\Omega + Q_\Lambda^\Omega, \quad (11)$$

with the terms

$$E_m = \int dV \varrho_0 \frac{v_m^2}{2},$$

$$Q_C = - \int dV (r \sin \theta)^2 \varrho_0 \mathbf{v}_m \cdot \text{grad} \frac{\Omega^2}{2},$$

$$\begin{aligned}
 Q_\nu^m = & - \int dV \frac{1}{2} [R_{rr} E_{rr} + 2R_{r\theta} E_{r\theta} + R_{\theta\theta} E_{\theta\theta} \\
 & + R_{\phi\phi} E_{\phi\phi}],
 \end{aligned}$$

$$Q_B^m = \int dV v_r \varrho_0 g \frac{s_1}{\gamma},$$

$$E_\Omega = \int dV \frac{1}{2} \varrho_0 (r \sin \theta)^2 (\Omega^2 - \Omega_0^2),$$

$$Q_\nu^\Omega = - \int dV \nu_t \varrho_0 (r \sin \theta)^2 \left[ \left( \frac{\partial \Omega}{\partial r} \right)^2 + \left( \frac{1}{r} \frac{\partial \Omega}{\partial \theta} \right)^2 \right],$$

$$Q_\Lambda^\Omega = - \int dV \nu_t \varrho_0 r \sin \theta \left( \frac{\partial \Omega}{\partial r} \Lambda_{r\phi} + \frac{1}{r} \frac{\partial \Omega}{\partial \theta} \Lambda_{\theta\phi} \right). \quad (12)$$

Here

$$\int dV = 4\pi \int_{r_{min}}^{r_{max}} dr \int_0^{\pi/2} d\theta r^2 \sin \theta \quad (13)$$

denotes the integral over the entire volume of the sphere from  $r = r_{min}$  to  $r = r_{max}$ . We emphasize that we solve our model only for the northern hemisphere but we compute from that the energy conversion for the entire sphere.  $E_m$  and  $E_\Omega$  denote energy available in the reservoir of meridional flow and differential rotation, respectively. For the latter we subtracted the core rotation rate to obtain a value representative for the differential rotation rather than total rotation.  $Q_C$  denotes the amount of energy that is converted by means of the Coriolis force (which is a sink for differential rotation and source for

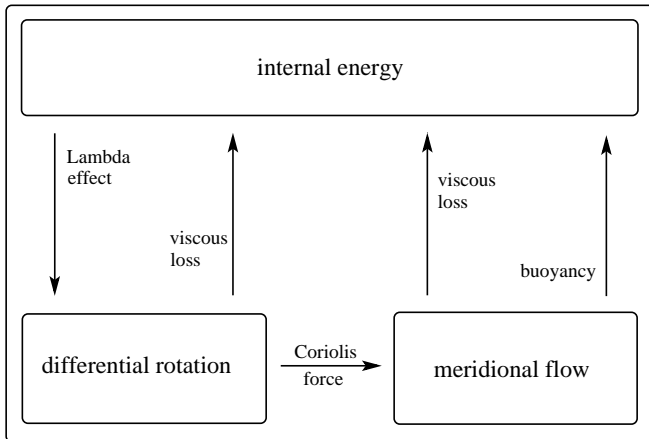


FIG. 4.— Schematic view of energy fluxes in differential rotation model.

meridional flow). The terms  $Q_\nu^m$  and  $Q_\nu^\Omega$  represent the losses through viscous dissipation for meridional flow and differential rotation, respectively.  $Q_\Lambda^\Omega$  is the energy which is converted through the  $\Lambda$ -effect from internal energy to energy of differential rotation, and  $Q_B^m$  denotes the work of the meridional flow against the buoyancy force arising from the entropy perturbation within the convection zone.

For the stationary reference model we can write the energy balance as:

$$Q_C = -Q_{visc}^m - Q_B^m, \quad (14)$$

$$Q_\Lambda^\Omega = -Q_{visc}^\Omega + Q_C, \quad (15)$$

where the left-hand side terms are the sources and the right-hand terms the sinks for the reservoirs of meridional flow and differential rotation, respectively. Figure 4 shows a qualitative diagram indicating the energy fluxes between the different energy reservoirs. A quantitative analysis of the model 1 of Rempel (2005), which we used in this paper as reference model, leads to

$$\begin{aligned} E_\Omega &= 1.55 \times 10^{33} \text{ J}, \\ Q_\Lambda^\Omega &= 6.6 \times 10^{24} \text{ W} = 0.017 L_\odot, \\ \tau_\Omega &= \frac{E_\Omega}{Q_\Lambda^\Omega} = 7.5 \text{ years}, \\ Q_\nu^\Omega &= -0.54 Q_\Lambda^\Omega, \\ Q_C &= 0.46 Q_\Lambda^\Omega \end{aligned} \quad (16)$$

for the differential rotation and to

$$\begin{aligned} E_m &= 10^{29} \text{ J}, \\ Q_C &= 3 \times 10^{24} \text{ J} = 0.008 L_\odot, \\ \tau_m &= \frac{E_m}{Q_C} = 9.4 \text{ hours}, \\ Q_\nu^m &= -0.02 Q_C, \\ Q_B^m &= -0.98 Q_C \end{aligned} \quad (17)$$

for the meridional flow.

In order to maintain the differential rotation in this model, the  $\Lambda$ -effect has to convert an amount of energy equivalent to around 1.7% of the solar luminosity. Comparing this energy flux to the energy stored in the reservoir of differential rotation leads to a time scale of around

8 years for the replenishment of energy. Around 54% of the energy converted by the  $\Lambda$ -effect returns directly to the reservoir of internal energy through viscous dissipation, while 46% flows through the action of the Coriolis force into the reservoir of meridional flow. Dividing the energy in this reservoir by the energy flux related to the Coriolis force leads to a time scale for the replenishment of energy in the meridional flow of only 10 hours, which is around a factor of 6500 shorter than the corresponding time scale for the differential rotation. The direct viscous loss does not play an important role for the meridional flow (only around 2% of the energy is dissipated); most of the energy returns to the reservoir of internal energy through work against the buoyancy force.

The numbers presented here vary with different model assumptions made but the fact that  $\tau_\Omega$  is around 4 orders of magnitude longer than  $\tau_m$  is a very robust result, since it follows mainly from the different sizes of the energy reservoirs of differential rotation and meridional flow. Another very robust result is that the viscous dissipation does not play an important role for the meridional flow (unless the assumed turbulent viscosity would be more than one order of magnitude larger than the value of  $5 \times 10^8 \text{ m}^2 \text{ s}^{-1}$  used here). This emphasizes the importance of the pole-equator entropy variation for avoiding the Taylor-Proudman state, as discussed in Rempel (2005), since the work of the meridional flow against the buoyant force is the primary sink of energy.

From the very short response time scale of  $\tau_m \sim 10$  hours it can be expected that the meridional flow is affected nearly instantaneously by fluctuations in the Reynolds stress, while the differential rotation only responds to a long term average over several years. As a consequence, the relative amplitudes of fluctuations in meridional flow and differential rotation are expected to scale with a factor of  $\sim \sqrt{\tau_\Omega/\tau_m} \sim 80$ , which is seen in the results presented before.

An order of magnitude estimate based on the energy yields:

$$\Delta E_m \sim v_{\text{rms}}^m \Delta v_{\text{rms}}^m, \quad (18)$$

$$\Delta E_\Omega \sim v_{\text{rms}}^\Omega \Delta v_{\text{rms}}^\Omega. \quad (19)$$

Given the fact that the amount of energy transferred into the meridional flow is roughly half the energy transferred into the differential rotation, the expected change in the flow amplitudes scales like

$$\frac{\Delta v_{\text{rms}}^m}{\Delta v_{\text{rms}}^\Omega} \sim \frac{1}{2} \frac{v_{\text{rms}}^\Omega}{v_{\text{rms}}^m} \sim 100, \quad (20)$$

(with  $v_{\text{rms}}^\Omega \sim 1 \text{ km s}^{-1}$  and  $v_{\text{rms}}^m \sim 5 \text{ m s}^{-1}$ . This is close to the ratio we obtained in the more detailed analysis of the energy fluxes within the model.

Since the large kinetic energy reservoir of the differential rotation tends to average fluctuations, a systematic variation of  $\sigma_\Omega$  with correlation time scale and length scale is seen in the data (longer lasting, large scale perturbations manifest easier in the differential rotation). On the other hand, the meridional flow shows a nearly immediate response to changes in the Reynolds stress. Therefore  $\sigma_v$  is mainly determined by the amplitude of the random fluctuations in the Reynolds stress assumed and not by the correlation time and length scale (unless the time scale for fluctuations in the Reynolds stress is

much shorter than  $\tau_m$ , which is not reasonable in the bulk of the convection zone). The only exception is the resonance found in case 2, which enhances the amplitude by about 50%.

## 5. CONCLUSIONS

We presented a mean field model for differential rotation and meridional flow including stochastic fluctuations in the Reynolds stress driving the differential rotation. We found that the variations in the differential rotation are around two orders of magnitude less than the variability observed in the meridional flow pattern. For example the case 3 discussed above shows a  $1\sigma$  variation of the 4 month mean of less than 0.3% of the rotation rate for the differential rotation (in latitudes lower than  $50^\circ$ ), while the  $1\sigma$  variation for the meridional flow is around 8% of the mean flow value (4 month mean) or even 20% of the mean flow value if also the short term variation is considered. The maximum amplitude of the short term meridional flow variability in this models is around  $10\text{ms}^{-1}$  and therefore close to 100% of the mean flow.

This result is a consequence of different response time scales of the differential rotation and meridional flow to changes in the Reynolds stress. Our model shows that the energy flows through the reservoir of differential rotation and meridional flow are comparable, while the kinetic energy of differential rotation exceeds that of meridional flow by about 4 orders of magnitude. As a consequence the meridional flow shows a nearly instantaneous response (on a time scale of less than a day) to changes in the Reynolds stress, while the differential rotation is

affected only by changes that have a long term average of at least 10 years.

Our result is in agreement with observations, which indicate that the  $1\sigma$  variation of the 4 month differential rotation inversions is a few nHz, but also show that the variations in the meridional flow can be of up to  $10\text{ms}^{-1}$ . However, most of the meridional flow measurements so far only address long term variability (time scale of years) rather than short term variability, which is the main focus of the model presented here.

We conclude that a fairly significant amount of random noise in the Reynolds stresses driving differential rotation can be tolerated without leading to variations in the differential rotation contradicting helioseismic inversions. However, the meridional flow will show significant variability on the same order of magnitude as the fluctuations of the Reynolds stress.

We found that the random forcing through the Reynolds stress excites inertia oscillations for times scales  $\tau_c \sim 1 - 2\Omega_0^{-1} \sim 4 - 8$  days. This resonance enhances the total variance  $\sigma_v$  by about 50% and has a visible but much weaker effect on  $\sigma_\Omega$ . However, this effect is not visible if the variance of the four month mean is considered. Therefore this effect could be observable in the variability of daily flow maps of the surface meridional flow but not in helioseismic inversions normally considering longer averages.

The author thanks P. A. Gilman for stimulating discussions and helpful comments on a draft of this manuscript and the anonymous referee for a helpful review.

## REFERENCES

- Brun, A. S. & Toomre, J. 2002, *ApJ*, 570, 865  
 Küker, M. & Stix, M. 2001, *A&A*, 366, 668  
 Kitchatinov, L. L. & Rüdiger, G. 1993, *A&A*, 276, 96  
 —. 1995, *A&A*, 299, 446  
 Miesch, M. S., Elliott, J. R., Toomre, J., Clune, T. L., Glatzmaier, G. A., & Gilman, P. A. 2000, *ApJ*, 532, 593  
 Rempel, M. 2005, *ApJ*, 622, 1320  
 Rüdiger, G., von Rekowski, B., Donahue, R. A., & Baliunas, S. L. 1998, *ApJ*, 494, 691  
 Schou, J., Howe, R., Basu, S., Christensen-Dalsgaard, J., Corbard, T., Hill, F., Komm, R., Larsen, R. M., Rabello-Soares, M. C., & Thompson, M. J. 2002, *ApJ*, 567, 1234  
 Zhao, J. & Kosovichev, A. G. 2004, *ApJ*, 603, 776